clustering proves to be a common effect in amphiboles, it will almost certainly preclude any widespread use of the infrared absorption method in cation-ordering studies.

ELECTRONIC ABSORPTION SPECTROSCOPY OF AMPHIBOLES

When light passes through a crystal containings a transition-metal ion, certain wavelengths are absorbed by excitation of electrons between the nondegenerate $3d$-orbital energy-levels. As the character and amount of separation of the orbital energy-levels are a function of the potential field applied by the crystal, occupancy of the different sites in a crystal will produce absorption of different wavelengths of light. Hence, electronic absorption spectra can be used to characterize site occupancy in crystals both qualitatively (by observation and assignment of spectral bands to specific cations in specific sites: Burns 1970a) and quantitatively (by comparison of intensities of spectral bands: Burns 1970b). This method is not straight-forward; the interpretation of the spectra is not easy, as illustrated by the work on the orthopyroxenes (White & Keester 1966, 1967, Bancroft & Burns 1967, Burns 1969, Runciman et al. 1973, Goldman & Rossman 1976, 1977b). The spectra may also be complicated by inter-element electron-transitions (Burns 1981), i.e., intervalence charge-transfer bands (IVCT), where transitions are from cation to anion, anion to cation or cation to cation. These transitions are particularly common where adjacent cations have variable valence states (e.g., Fe^{2+} and Fe^{3+}, Ti^{3+} and Ti^{4+}, Fe^{2+} and Ti^{4+}) and are a major cause of color and pleochroism in amphiboles (Manning & Nickel 1969, Faye & Nickel 1970, Strens 1970). The intensity of this type of band is about two orders of magnitude larger than the intensity of normal $d-d$ transitions. Thus overlap of these two types of band in an absorption spectrum can obscure the $d-d$ transition bands. The occurrence of more than one type of transition-metal cation in the structure, as is common in most amphiboles, will further complicate the interpretation of the absorption spectra. For the derivation of quantitative site-occupancies, additional problems arise. The intensity of an absorption is a function of the probability of occurrence of the transition. The transition probability is governed by the Laporte selection rule (King 1964), which forbids transitions between $3d$ orbitals. When a transition-metal cation occupies a site without a centre of

symmetry, mixing of the $3d$ and $4p$ orbitals allows a transition, the intensity of which is a function of the degree of $3d-4p$ mixing that is, in turn, related to the deviation of the cation environment from centrosymmetry. Thus when a transition-metal cation occurs in more than one site in a crystal, the intensities of the $d-d$ bands are a function of both the cation occupancies and the deviation of the cation environment from centrosymmetry. In centrosymmetric sites, some $3d-4p$ orbital mixing may occur by vibronic coupling, and hence very weak bands can result from cations in these sites. Local disorder can also give rise to intensification of $d-d$ bands in solid solutions; Robbins & Strens (1972) have noted this effect in micas and termed it "substitutional intensification". This could lead to nonlinear relationships in Beer's-law-type plots. These arguments suggest that calibration may be a problem for quantitative site-occupancy derivation. Conversely, this technique potentially has a qualitative sensitivity that the other common techniques lack.

Early work on amphiboles include that of Melankholin (1956), Chesnokov (1961). Littler & Williams (1965) and White & Keester (1966); these studies illustrated the importance of charge transfer on the pleochroism of amphiboles but encountered difficulties in the assignment of $d-d$ bands. The last decade has seen great improvements in instrumentation, experimental technique and interpretation; this has been greatly aided by our increased understanding of the crystal chemistry of amphiboles and the co-operative use of other techniques; a general survey of the results follows.

Fe–Mg–Mn amphiboles

Mao & Siefert (1974) reported the polarized electronic absorption spectra of anthophyllite and gedrite (these are, respectively, anthophyllite[23] and gedrite[32] of Appendix C); the spectra are shown in Figure 87. The anthophyllite spectra are dominated by an intense band at $\sim$10800 cm^{-1} that is particularly intense in the β spectrum and a broad intense band at $\sim$4200 cm^{-1} that is particularly intense in the α spectrum. These are assigned to $d-d$ transitions in Fe^{2+} at the M4 site; the predominance of these bands is a result of the very noncentrosymmetric configuration of the environment about the M4 site that allows violation of the Laporte selection rule. The polarization characteristics of these bands are also compatible with this assignment. The remaining features of the spectra are much less intense. The sharp spike in the α spectrum at
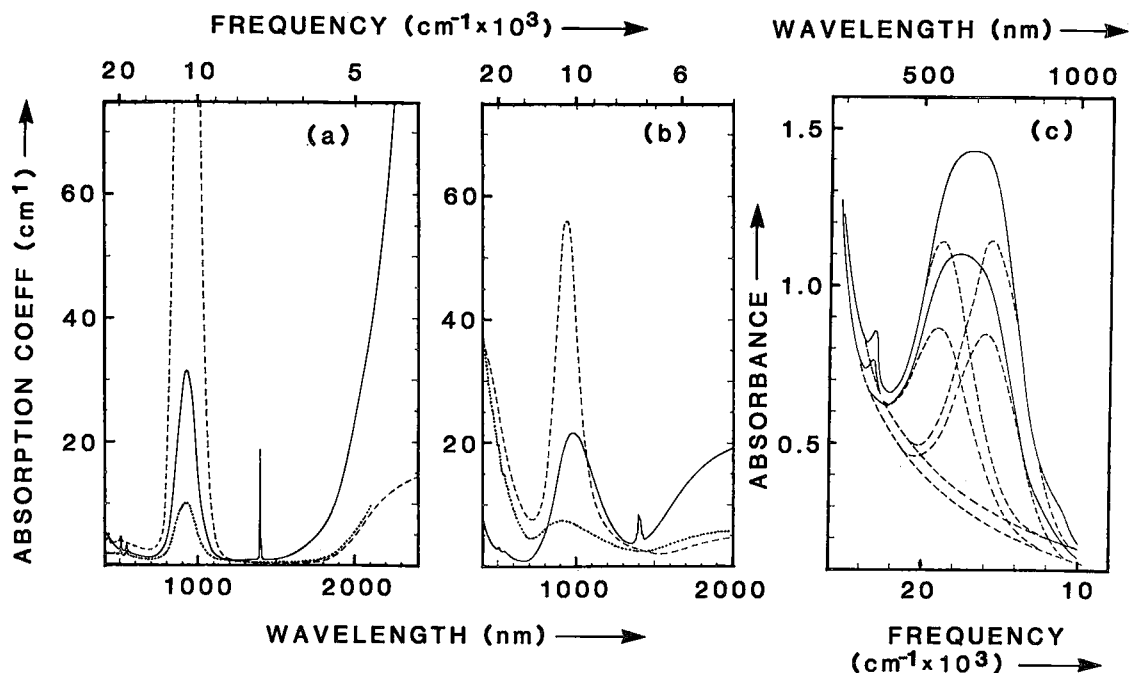
FIG. 87. Polarized electronic absorption spectra for anthophyllite (left) and gedrite (centre), from Mao & Seifert (1974), and holmquistite (right), from Faye & Nickel (1970).

~ 7300 cm^{-1} is an overtone of the principal OH stretch. There are several minor bands in the region 17000–23000 cm^{-1}; these are assigned to spin-forbidden transitions in Fe^{2+}. The gedrite spectra are fairly similar to those of anthophyllite. They are also dominated by intense bands at ~ 10800 cm^{-1} in β and ~ 4500 cm^{-1} in α that can be assigned to d–d transitions in Fe^{2+} at M4; however, these bands are significantly weaker than in anthophyllite in response to the more regular M4 environment in gedrite. These bands are also broader than in anthophyllite, presumably the result of substitutional broadening. The strong sloping absorption in the gedrite spectra in the region >15000 cm^{-1} results from the presence of Fe^{3+} in the structure, causing the migration of the metal–ligand charge-transfer band into the visible region.

The spectra of holmquistite were reported by Faye & Nickel (1970) and are shown in Figure 87. There is an intense charge-transfer band in the 12000–20000 cm^{-1} region of the β and γ spectra. There is also a spin-forbidden Fe^{3+} band at ~ 22800 cm^{-1} and a weak spin-allowed Fe^{2+} d–d band at ~ 108000 cm^{-1} in the γ spectrum. Faye & Nickel (1970) chose to deconvolute the major absorption into two

bands that they assigned to Fe$^{2+}_{M(1)}$ $\rightarrow$ Fe$^{3+}_{M(3)}$ and Fe$^{2+}_{M(1)}$ $\rightarrow$ Fe$^{3+}_{M(2)}$ interactions, respectively. This assignment is rather unlikely, considering the cation arrangement and configuration in this amphibole (Irusteta & Whittaker 1975, Law 1973, Appendices C3 and F). The β spectrum should have two Fe^{2+}–Fe^{3+} IVCT bands of approximately equal intensity: Fe$^{2+}_{M(3)}$ $\rightarrow$ Fe$^{3+}_{M(2)}$ and Fe$^{2+}_{M(1)}$ $\rightarrow$ Fe$^{3+}_{M(2)}$; the γ spectrum should have a single Fe^{2+}–Fe^{3+} IVCT band approximately equal in intensity to the composite band in the β spectrum: Fe$^{2+}_{M(1)}$ $\rightarrow$ Fe$^{3+}_{M(2)}$.

Burns (1970a) has presented spectra for cummingtonite and grunerite, and Goldman (1979) has reported the spectra of grunerite; the spectra are shown in Figure 88. The prominent bands at ~ 10000 cm^{-1} in β and ~ 4000 cm^{-1} in α are assigned to d–d transitions in Fe^{2+} at the M(4) site. Also common to both spectra are the sharp but weak spin-forbidden Fe^{2+} bands in the 18000–21000 cm^{-1} region and the fine-structure overtones of the principal OH stretch around 7100 cm^{-1}. In the cummingtonite spectra, there is a very weak band at ~ 8400 cm^{-1}; this becomes much more prominent in the α and γ spectra of grunerite. Both the compositional dependence of the intensity
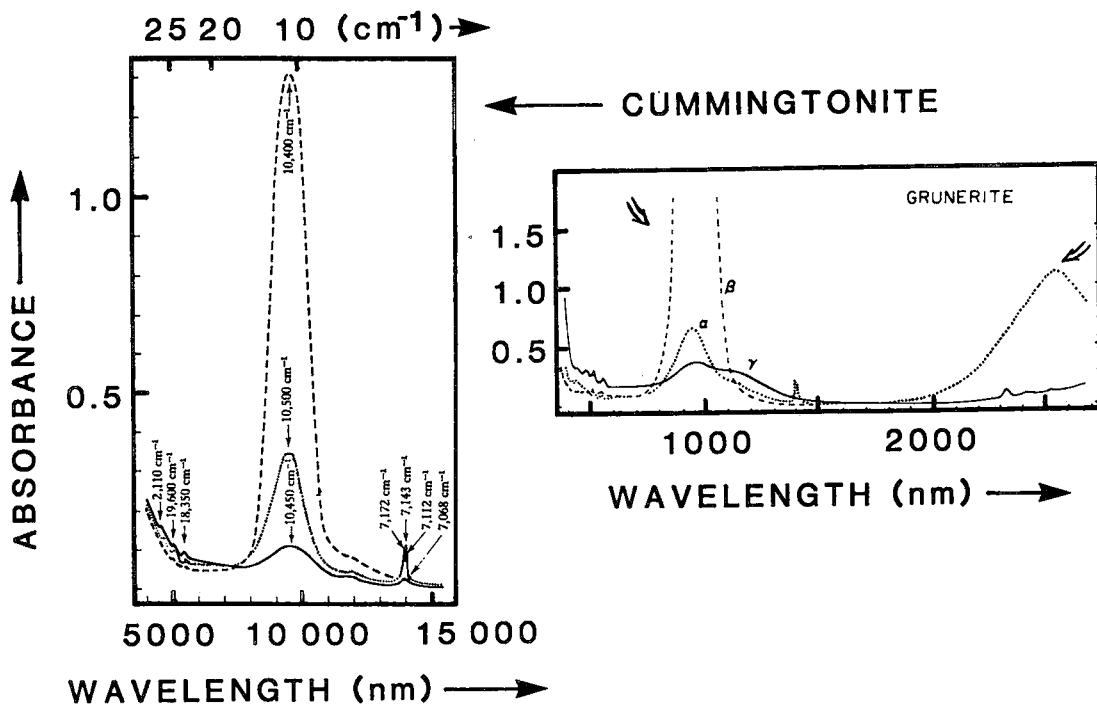
FIG. 88. Polarized electronic absorption spectra of cummingtonite (left) and grunerite (right) [from Burns (1969, 1970a) and Goldman (1979), respectively]; ... α spectrum. - - - β spectrum. ——— γ spectrum.

and the position (by analogy with the ortho-pyroxene and pigeonite spectra) suggest that this may be assigned to a *d–d* transition in Fe^{2+} at the M(1), M(2) and M(3) sites; as the environment of M(2) is more noncentrosym-metric than those of M(1) and M(3), this should primarily be due to Fe^{2+} at M(2). Comparison with the spectrum of hedenbergite (Rossman 1980) suggests that other *d–d* bands due to Fe^{2+} at M(1), M(2) and M(3) may be incor-porated into the major absorption bands at ~ 10200 cm^{-1}.

Calcic amphiboles

Spectra for amphiboles of the tremolite – ferro-actinolite series were reported by Burns (1969, 1970a) and Goldman & Rossman (1977a), and are shown in Figure 89. Both the tremolite and the actinolite spectra are dominated by an intense band located at ~ 9800 cm^{-1} and both have a prominent broad band in the α spectrum at ~ 4200 cm^{-1}. After the tremolite of Figure 89 had been heated (in air at 535°C for 8 hours), the major spectral change found was a decrease in intensity of $\sim 50\%$ of *both* the 9800 and 4200 cm^{-1} bands; this suggests that these bands originate from the same (Fe^{2+})

cation. The similarity of the ~ 9800 cm^{-1} band to bands in the spectra of the Fe–Mg–Mn amphiboles (Figs. 87 and 88) and the ortho-pyroxenes (Burns 1970a, Runciman *et al.* 1973, Goldman & Rossman 1976, 1977b), together with the great intensity of this band, suggests that it is due to Fe^{2+} at the M(4) site. Further-more, Goldman & Rossman (1977a) showed that this band was present in tremolite and actinolite, where the sum of the C-type cations exceeds 5.00; and hence some small cation (Fe^{2+}, Mg, Mn) occupancy of the M(4) site is inferred to have occurred, but was not present in the spectra of a pargasite, where the sum of the C-type cations is approximately 5.00 and no small cation occupancy of the M(4) site was required by the stoichiometry. This interpretation of the 10000 cm^{-1} band as being due solely to Fe^{2+} at M(4) has been challenged by Aldridge *et al.* (1982). These authors used EHMO calculations to derive the 3*d* electronic energies in a series of simple structures, and empirically related the calculated energies to the observed electronic energies. Applying this method to grunerite confirms that the 4000 cm^{-1} band is due to Fe^{2+} at M(4), but also indicates that the 10000 cm^{-1} band is a compo-
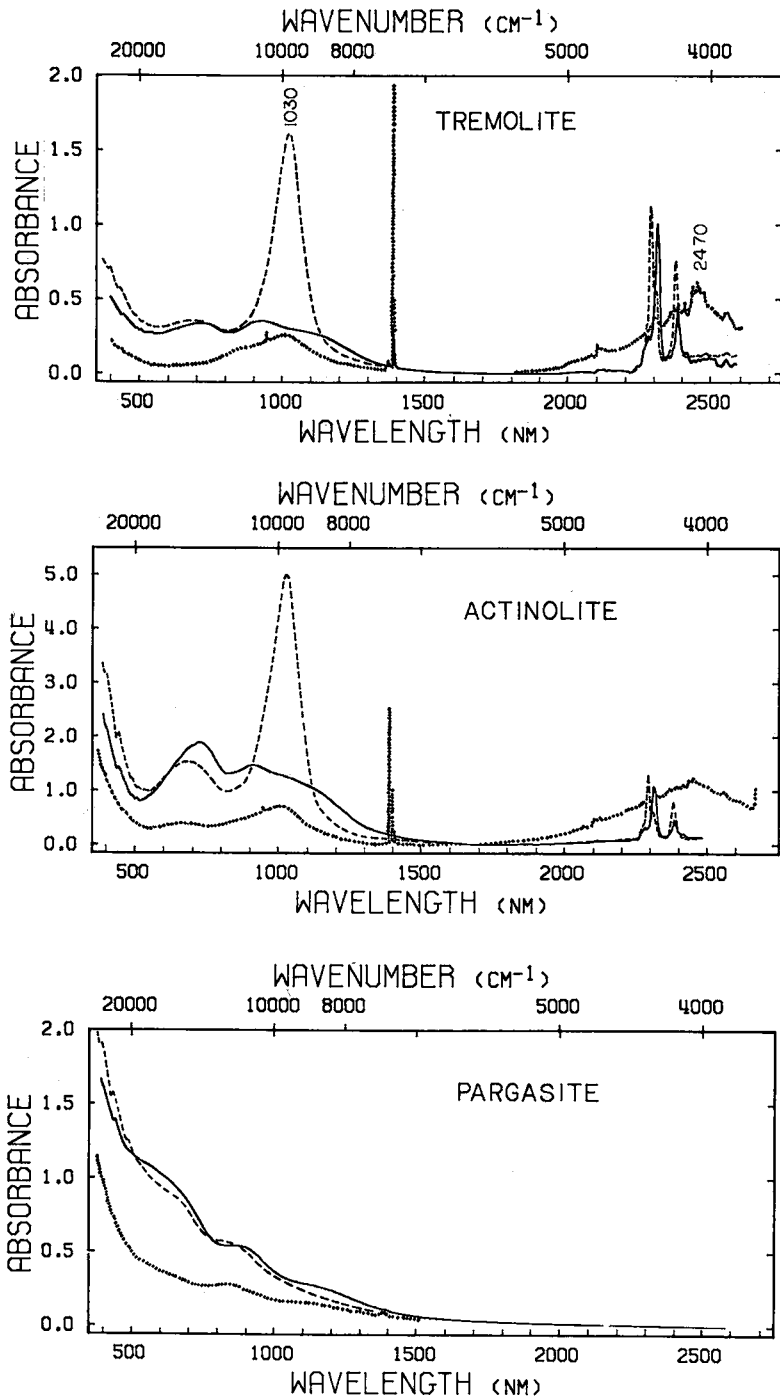
FIG. 89. Polarized electronic absorption spectra of tremolite (top), actinolite (centre) and pargasite (bottom) [from Goldman & Rossman (1977)]; ... α spectrum, - - - β spectrum, ———— γ spectrum.

site due to Fe^{2+} at M(1), M(2), M(3) and M(4). The M(1) and M(3) octahedra are fairly regular, and thus Fe^{2+} at these sites will not contribute significantly to the 10000 cm^{-1} band. Thus far, this argument seems reasonable, and the point of contention is whether or not Fe^{2+} at M(2) contributes significantly to the 10000 cm^{-1} band. Aldridge *et al.* (1982) cited the differential intensity of the 10000 cm^{-1} band in cummingtonite and grunerite (with similar amounts of Fe^{2+} at the M(4) site) as evidence of significant M(2) contribution in grunerite. They suggested that molar absorptivity values at M(2) could be ~½ the corresponding values at M(4). This would not seem to be reasonable from the geometry of the M(2) and M(4) environments. Their argument assumes that the molar absorptivity value for Fe^{2+} at M(4) does not change across the cummingtonite – grunerite series. The average environment of the M(4) site becomes more distorted with increasing enrichment in iron across the series (Fig. 68). A probe of the local environment around Fe^{2+} at M(4) is provided by the quadrupole-splitting parameter from Mössbauer spectroscopy. As shown in Figure 67, the quadrupole splitting strongly decreases with increasing Fe^{2+} p.f.u., indicating that the local environment around Fe^{2+} at M(4) becomes more distorted across the series from cummingtonite to grunerite. Thus some of the increase in molar absorptivity of the 10000 cm^{-1} band can be ascribed to increasing transition probability of Fe^{2+} at the M(4) site. This would suggest that Fe^{2+} at M(2) does not contribute to the 10000 cm^{-1} as much as suggested by Aldridge *et al.* (1982). However, it does *not* show that such a contribution is negligible. Goldman & Rossman (1982) showed that the intensities of the 10000 cm^{-1} and 4500 cm^{-1} bands are strongly correlated in a series of calcic and Fe–Mg–Mn amphiboles; however, such a correlation would occur if Fe^{2+} at M(2) contributed significantly to the 10000 cm^{-1} band, provided there was a regular distribution of Fe^{2+} over the M(2) and M(4) sites. The same argument applies to the correlation between the Fe^{2+} content of M(4) derived from Mössbauer results and the intensity of the 10000 cm^{-1} band. Thus at the moment, the significance of an M(2) Fe^{2+} contribution to the 10000 cm^{-1} band is unclear. Perhaps the solution to this problem may be found by relating known molar-absorptivity values to polyhedron distortion for a series of simple structures, and then apply this empirical relationship to the amphibole structure.

Weak spin-forbidden Fe^{2+} and Fe^{3+} transitions occur from ~18000 to 23000 ccm^{-1} (Fig. 89), and the overtone of the principal OH stretch is prominent at ~7300 cm^{-1}. Bands at ~15200 cm^{-1} in β and ~13800 cm^{-1} in γ may be assigned to $Fe^{2+} - Fe^{3+}$ IVCT bands (in the absence of Cr^{3+}); note the absence of any comparable band in the α spectrum where there is no component of a $^{M4}Fe^{2+}-^{M4}Fe^{3+}$ separation parallel to the electric vector. The broad weak bands between 8000 and 12000 cm^{-1} in the γ spectrum are probably *d–d* transitions of Fe^{2+} at the M(1), M(2) and M(3) sites, particularly the M(2) site. The fine structure in the region of ~4200 cm^{-1} can be attributed to infrared combination-modes, as shown by Burns & Strens (1966).

Goldman & Rossman (1977a) also reported the spectrum of pargasite. As shown in Figure 89, this lacks the prominent bands at ~10200 cm^{-1} in β and ~4200 cm^{-1} in α that are characteristic of Fe^{2+} at M(4); this is in agreement with the stoichiometry of this particular amphibole, which indicates no excess of C-type cations. Weak bands in the 8000–13000 cm^{-1} region are most probably *d–d* transitions of Fe^{2+} at M(1), M(2) and M(3), and weak spin-forbidden Fe^{2+} and Fe^{3+} bands occur above ~20000 cm^{-1}. In the β and γ spectra are broad bands at ~15000 cm^{-1}; their positions and polarization dependence suggest that they are $Fe^{3+}-Fe^{2+}$ IVCT bands, but they are surprisingly weak compared with corresponding bands in other amphibole spectra. The wing of the ultraviolet charge-transfer band extends well into the visible region in the β and γ spectra, presumably the result of significant Fe^{3+} at the M(2) site.

Goldman (1977) has shown that the intensity of the bands at ~14000 cm^{-1} (in β and γ) that are generally assigned to $Fe^{2+} \rightarrow Fe^{3+}$ charge transfer correlate well with the Fe^{3+} concentration in three calcic amphiboles. If this is more generally the case, this should prove a powerful method for deriving Fe^{3+}/Fe^{2+} ratios when used in conjunction with results of electron-microprobe analyses. The arguments of Bakhtin & Vinokurov (1978), who interpreted these bands in amphiboles (and other silicates) as electric-dipole transitions in exchange-coupled $Fe^{2+}-Fe^{3+}$ pairs from the $^{5}T_{2}{}^{6}A_{1}$ ground state to the $^{5}T_{2}{}^{4}T_{2}$ excited state, should not affect the utility of this method.

Sodic–calcic amphiboles

Faye & Nickel (1970) reported the spectra of potassian ferri-taramite ("ferro-hastingsite" in
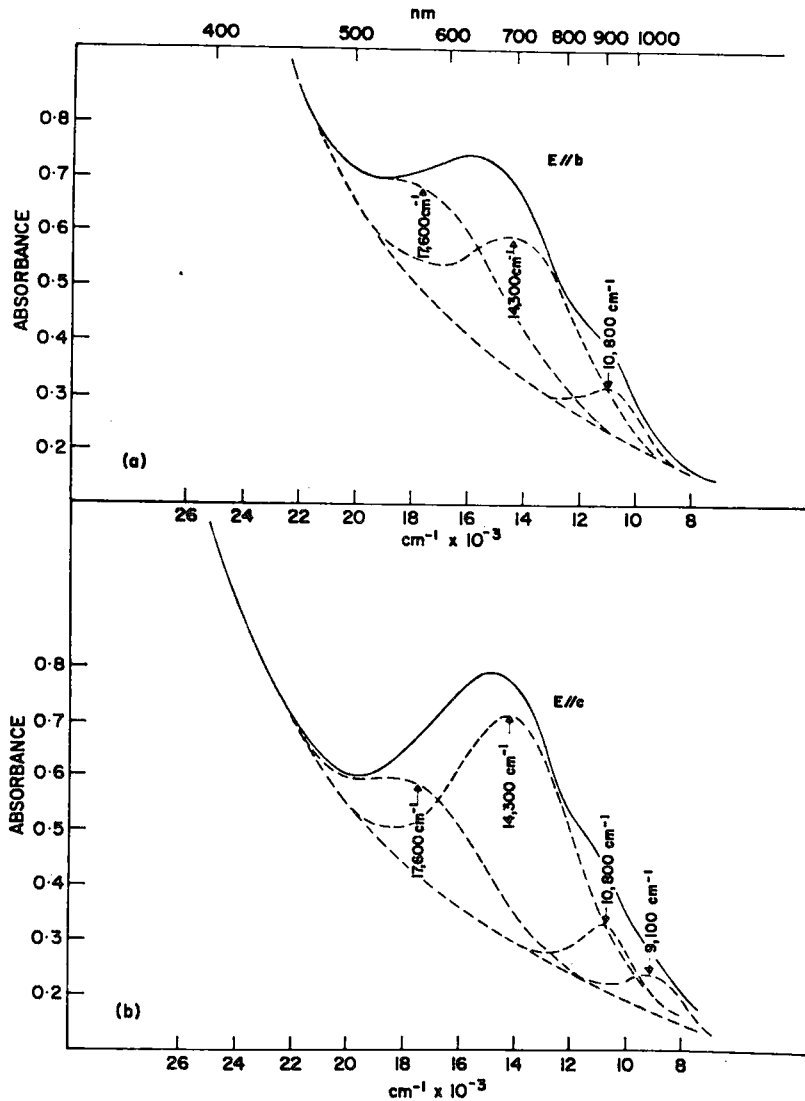
FIG. 90. Polarized electronic absorption spectra of potassian ferri-taramite [from Faye & Nickel (1970)].

their study; this is the potassian ferri-taramite(59) of Appendix B); the spectra are shown in Figure 90. They are dominated by broad asymmetric bands centred on ~ 16000 cm^{-1} and ~ 15000 cm^{-1} in the β and γ spectra, respectively. Their polarization dependence, position and intensity show these to be intervalence charge-transfer bands. There is a prominent shoulder at ~ 10800 cm^{-1} in both the β and the γ spectra, with possibly a secondary shoulder in the γ spectrum at ~ 9100 cm^{-1}. These may be assigned to d–d

transitions of Fe^{2+}; without the α spectrum at lower wavelengths, it would be premature to assign these to Fe^{2+} at any specific site. Faye & Nickel (1970) deconvoluted the IVCT band into two component bands at ~ 17600 cm^{-1} and 14300 cm^{-1}, assigning these to Fe^{2+}$_{M(1)}$ $\rightarrow$ Fe^{3+}$_{M(3)}$ and Fe^{2+}$_{M(1)} \rightarrow$ Fe^{3+}$_{M(2)}$ interactions, respectively. This assignment is rather unlikely considering the cation arrangement and configuration in this amphibole (Appendix B3). However, these charge-transfer bands should be composite. The β spectrum should have two

Fe^{2+}–Fe^{3+} IVCT bands of approximately equal intensity: $Fe^{2+}_{(M3)} \rightarrow Fe^{3+}_{M(2)}$ and $Fe^{2+}_{M(1)} \rightarrow Fe^{3+}_{M(2)}$; the γ spectrum should have a single Fe^{2+}–Fe^{3+} IVCT band approximately equal in intensity to the resultant band in the β spectrum: $Fe^{2+}_{M(1)} \rightarrow Fe^{3+}_{M(2)}$. This amphibole also contains significant Ti and Mn, giving rise to the possibility of heteronuclear IVCT bands contributing to the major absorption. There are some problems in the IVCT band-assignments in this (and other) amphiboles examined in detail by Faye & Nickel (1970). The maximum absorption should occur when $E // Z$, as in this orientation there is maximum interaction between the electric vector of the incident radiation and the overlapping t_{2g} orbitals on adjacent Fe cations. Faye & Nickel showed that the direction of maximum absorption is actually inclined to the Z axis by up to $\sim 30°$. They proposed that this is accounted for by an "intensity borrowing mechanism", whereby the high-energy band at ~ 18000 cm^{-1} is enhanced by "borrowing intensity" from the very intense $O^{2-} \rightarrow Fe^{3+}$ charge-transfer band occurring in the UV region of the spectrum. As the direction of maximum absorption of the $O^{2-} \rightarrow Fe^{3+}$ charge-transfer process does not (necessarily) correspond with that of the $Fe^{2+} \rightarrow Fe^{3+}$ charge-transfer process, intensity borrowing will

perturb the direction of maximum absorption from that expected for an $Fe^{2+} \rightarrow Fe^{3+}$ charge-transfer band. Alternately, this may result from using convergent light, which mixes the polarization components of the absorption bands.

Alkali amphiboles

The spectra of glaucophane and riebeckite were reported by Bancroft & Burns (1969) and Faye & Nickel (1970), respectively; the spectra are shown in Figure 91. The glaucophane spectra are dominated by intense IVCT bands at ~ 18500 cm^{-1} and ~ 16100 cm^{-1} in β and γ, respectively. The γ band contains only a component of the $Fe^{2+}_{M(1)} \rightarrow Fe^{3+}_{M(2)}$ interaction, whereas the β band is due to both this and the $Fe^{2+}_{M(3)} \rightarrow Fe^{3+}_{M(2)}$ interaction; the β band is slightly asymmetric, suggesting an $Fe^{2+}_{M(1)} \rightarrow Fe^{3+}_{M(2)}$ component to its total intensity. The relative energies of the $Fe^{2+}_{M(1)} \rightarrow Fe^{3+}_{M(2)}$ and $Fe^{2+}_{M(3)} \rightarrow Fe^{3+}_{M(2)}$ interactions are as expected from their cation distances [M(1)–M(2) < M(2)–M(3)]. The spin-forbidden Fe^{3+} peak at ~ 22300 cm^{-1} and the OH-stretch overtones at ~ 7100 cm^{-1} also are present. The remaining weak bands between 8000 and 13000 cm^{-1} are d–d transitions of Fe^{2+} at M(1) and
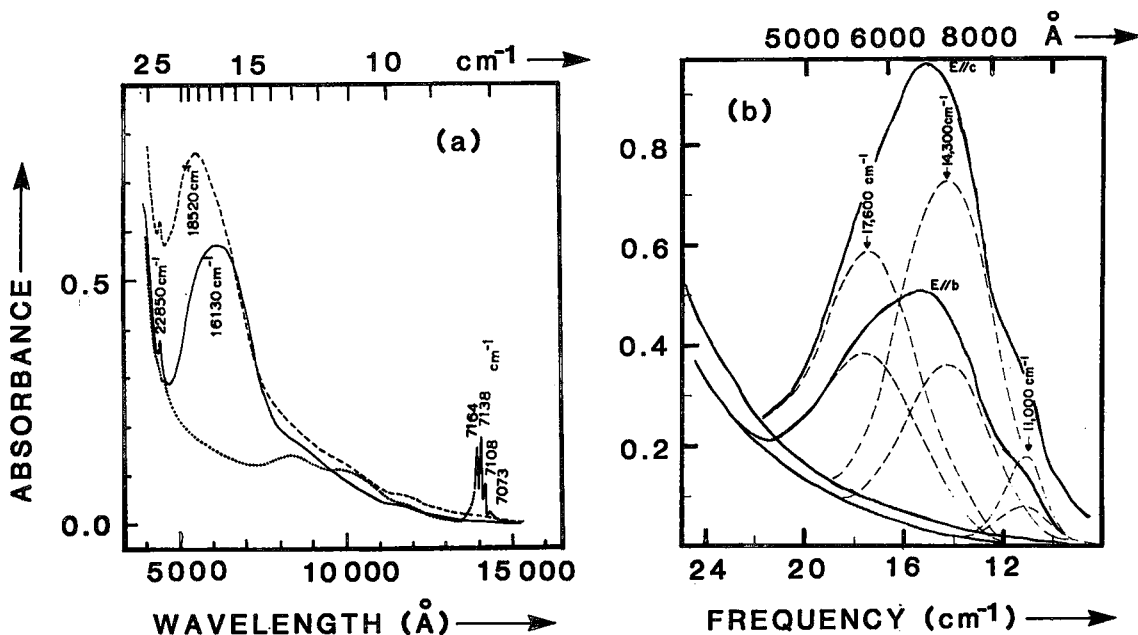

Fig. 91. Polarized electronic absorption spectra of glaucophane (left) and riebeckite (right) [from Bancroft & Burns (1969) and Faye & Nickel (1970)]. For glaucophane, ... α spectrum, - - - - β spectrum, ———— γ spectrum.

M(3). The spectrum of riebeckite is similar to that of glaucophane, being dominated by intense IVCT bands in the β and γ spectra. This is to be expected, as it is the riebeckite component in glaucophane that gives rise to the charge-transfer bands.

Effects of other transition metals

Other transition metals, particularly Mn, Ti and Cr, are common minor constituents in amphiboles. These will also contribute to the absorption spectra primarily through d–d transitions and heteronuclear IVCT transitions. The only work is by Neuhaus (1960) and Goldman (1977), who characterized the spectra of Mn and Cr in amphiboles. Figure 92 shows the spectra of a tremolite containing significant Mn. The wide bands in the 15000–20000 cm^{-1} region have been assigned to d–d transitions in Mn^{3+}, with the sharp bands in the 20000–25000 cm^{-1} region being spin-forbidden Mn^{2+} or Mn^{3+} transitions. Many amphiboles have prominent Fe^{2+}–Fe^{3+} IVCT bands around ~15000 cm^{-1}
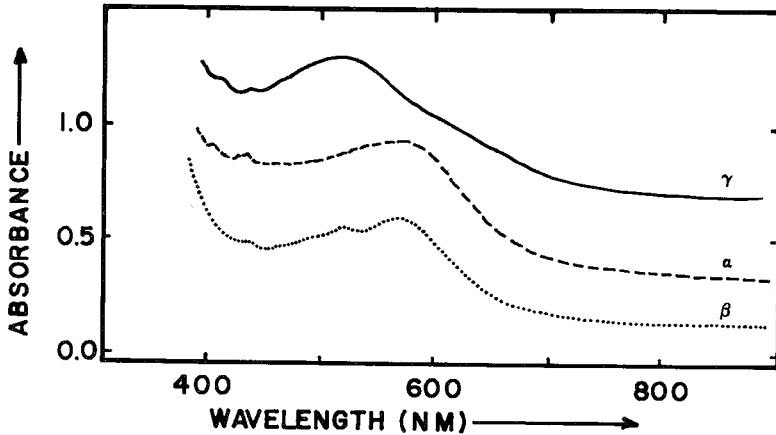

FIG. 92. Polarized electronic absorption spectra of Mn-containing tremolite [from Goldman 1977)].
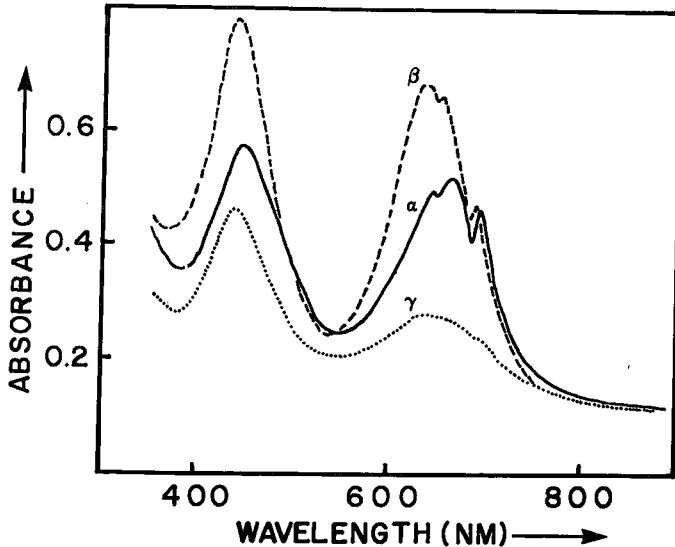

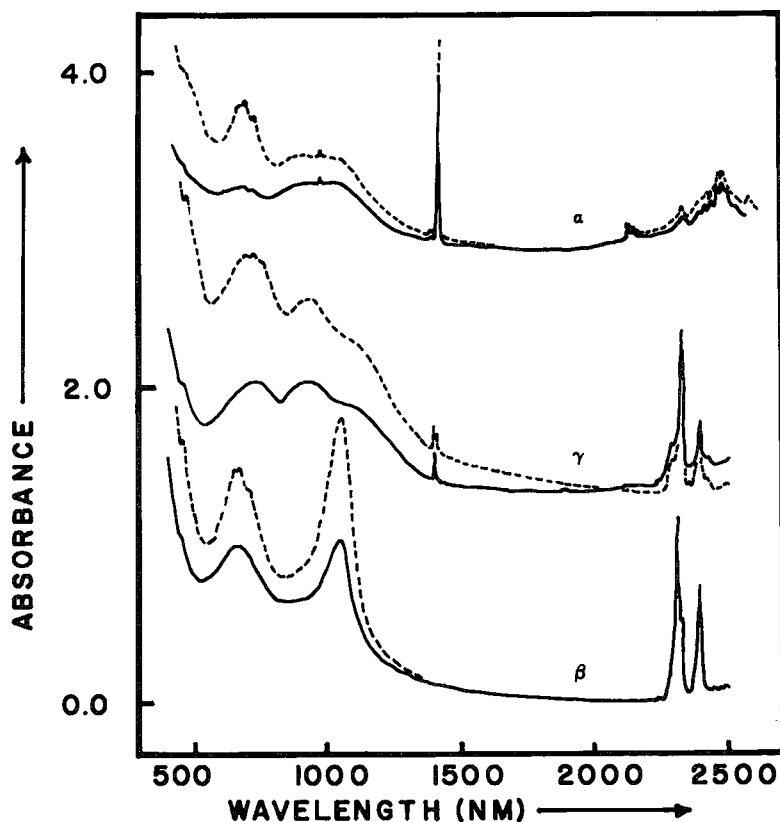FIG. 93. Polarized electronic absorption spectra of Cr-bearing tremolite [from Goldman (1977)].

FIG. 94. Polarized electronic absorption spectra of Cr-bearing actinolite [from Goldman (1977)].

in their β and γ spectra that will tend to obscure any Mn bands; however, these may be apparent in the α spectra. Figure 93 shows the spectra of a tremolite containing significant Cr^{3+}. The broad intense bands at ~ 15400 cm^{-1} and 22200 cm^{-1} are (spin-allowed) d–d transitions of Cr^{3+}, with the sharp bands at ~ 14400 cm^{-1} and ~ 14600 cm^{-1} being spin-forbidden transitions. Figure 94 shows the spectrum of an actinolite with significant Cr^{3+}. The bands at ~ 15400 cm^{-1} are definitely characteristic, particularly in the α spectrum; without the α spectrum, it is feasible that these could be confused with an Fe^{2+}–Fe^{3+} IVCT band.

MISCELLANEOUS SPECTROSCOPIC METHODS
AND AMPHIBOLES

The work summarized here has generally been exploratory in nature, and thus extensive characterization of amphiboles has not yet been done. Nevertheless, such studies indicate both the potential and the drawbacks of such methods

when examining materials as complex as amphiboles.

X-ray photoelectron spectroscopy

X-ray photoelectron spectroscopy (ESCA, electron spectroscopy for chemical analysis) may be used to examine relative core-binding energies (electron-orbital energy levels) of atoms in crystals. In principle, this technique should have wide application in studies on site-population characterization and chemical bonding in minerals, and early studies (Yin et al. 1971, Huntress & Wilson 1972) suggested that this might be the case. However, more extensive studies on a wide variety of silicate minerals (Adams et al. 1972) indicate that there are important limitations to this technique. Firstly, lines of paramagnetic ions (e.g., Fe^{2+} and Fe^{3+}) are very broad because of exchange interaction. No energy differences were observable between Fe $2P$ binding energies of Fe^{2+} (in hedenbergite) and Fe^{3+} (in epidote); in addition, there was no